Research in Basic Sciences: Results of some math and physics projects

Universidad Tecnológica de Pereira

Editorial UTP

Autores Varios

Research in Basic Sciences Results of some math and physics projects

Henry Riascos Landázuri
Juan David Lopez Vargas
Daniel Cortés Zapata
Alexander Gutiérrez Gutiérrez
Alberto García López

Universidad Tecnológica de Pereira

Vicerrectoría de Investigaciones, Innovación y Extensión
Facultad de Ciencias Básicas
Colección Trabajos de Investigación
2022

Research in basic sciences : Results of some math and physics projects / Henry Riascos Landázuri y otros. – Pereira : Editorial Universidad Tecnológica de Pereira, 2022.
58 páginas.

eISBN: 978-958-722-805-2

1. Películas delgadas (Física) 2. Microscopia de fuerza atomica 3. Electrónica del estado sólido 4. Galvanoplastia al vapor 5. Geometría descriptiva básica 6. Autocad

CDD. 530.4275

Research in Basic Sciences Results of some math and physics projects.

Publicación financiada con recursos de la Vicerrectoría de Investigaciones , Innovación y Extensión de la Universidad Tecnológica de Pereira

eISBN: 978-958-722-805-2

Imagen de cubierta tomada de: Freepik.

Universidad Tecnológica de Pereira
Vicerrectoría de Investigaciones, Innovación y Extensión
Editorial Universidad Tecnológica de Pereira
Pereira, Colombia

Coordinador editorial:
Luis Miguel Vargas Valencia
luismvargas@utp.edu.co
Teléfono 313 7381
Edificio 9, Biblioteca Central “Jorge Roa Martínez”
Cra. 27 No. 10-02 Los Álamos, Pereira, Colombia
www.utp.edu.co

Montaje y producción:
María Alejandra Henao Jiménez
Universidad Tecnológica de Pereira

Pereira, Risaralda, Colombia.

CONTENIDO

Introducción

En el marco del ***"Año Internacional de las Ciencias Básicas para el Desarrollo Sostenible" (International Year of Basic Sciences for Sustainable Development)*** propuesto por la UNESCO para el 2022, se busca destacar la importancia de las Ciencias Básicas, tales como la biología, física, la química y las matemáticas, en la creación de soluciones sostenibles para enfrentar los desafíos globales. El propósito de esta es iniciativa es promover la educación y la investigación en Ciencias Básicas a nivel mundial y la colaboración entre los científicos y organizaciones internacionales para abordar los desafíos globales como el cambio climático, la seguridad alimentaria, la energía, entre otros.

Estas disciplinas son fundamentales para el avance de la ciencia y la tecnología porque constituyen la base de muchas otras áreas del conocimiento, y sus descubrimientos y avances han tenido un impacto significativo en la sociedad. En las universidades, las Ciencias Básicas son una parte esencial de la formación de los estudiantes y futuros profesionales, ya que proporcionan las herramientas y el conocimiento necesarios para comprender y abordar los desafíos científicos actuales y futuros. Además, la investigación en Ciencias Básicas también es la base para el desarrollo de nuevas tecnologías y aplicaciones prácticas.

La innovación y el desarrollo en campos como la medicina, la energía, la informática, nuevos materiales, agroindustria, economía, ciudades inteligentes, maching learning, ciencias de los datos, ciencias de la información cuántica, la biotecnología, entre muchos otros, no serían posibles sin los avances en estas ciencias fundamentales. Los descubrimientos en biología molecular, por ejemplo, han llevado al desarrollo de nuevas terapias para enfermedades genéticas y cáncer. La física ha permitido avances en la tecnología de la energía, como la energía solar y la fusión nuclear, o los nuevos materiales nos permiten tener mayor capacidad de almacenamiento de información, o

tener mejores propiedades físicas y mecánicas como mayor resistencia o flexibilidad.

Desde nuestra Facultad se presentan trabajos resultados de investigación que le aportan significativamente a las aplicaciones de las ciencias básicas y que son el resultado del compromiso y la dedicación de nuestros docentes investigadores, quienes trabajan para abordar problemas complejos y generar soluciones innovadoras y sostenibles.

En el primer capítulo se presenta un estudio de las propiedades en nuevos materiales, en este caso del crecimiento de películas delgadas de grafeno en sustrato de silicio utilizando el método de deposición por láser pulsado (DLP) donde se utilizaron 6 técnicas de caracterización (Espectroscopía Raman, IRTF, MEB, SED, MFA, MACA) y como conclusión se tiene que las muestras similares al grafeno presentan propiedades de hidrofobicidad y las muestras de carbono amorfo tienen propiedades hidrofílicas.

En el segundo capítulo se presenta un modelamiento matemático y una discusión sobre la existencia de soluciones de segunda clase en una ecuación de Tricomi, se plantea la existencia de soluciones periódicas de una generalización de la ecuación de Tricomi, el estudio se realiza mediante métodos perturbativos; de igual forma, se usa la función de Melnikov para encontrar las condiciones bajo las cuales se conservan las curvas homoclínicas.

En el tercer capítulo se plantea una metodología de enseñanza-aprendizaje para enseñar la geometría descriptiva básica y la resolución de problemas a través del software Autocad.

Se agradece a todos los docentes, estudiantes, equipos de trabajo y colaboradores de la Facultad de Ciencias Básicas y a la Vicerrectoría de Investigaciones, Innovación y Extensión, por seguir aportando a la construcción y fortalecimiento de la ciencia, la tecnología y la innovación, a mejorar los procesos de formación y la aplicabilidad de las ciencias en diversos ámbitos y que impactan sin duda a una sociedad del conocimiento.

Juan Pablo Trujillo Lemus
Decano
Facultad de Ciencias Básicas
Universidad Tecnológica de Pereira

1 CAPÍTULO UNO

Study of graphene growth onto silicon substrates by pulsed laser deposition method

Estudio del crecimiento de grafeno en sustratos de silicio usando el método de deposición por láser pulsado

Henry Riascos Landázuri[1] and Juan David Lopez Vargas[2]

Abstract

This chapter presents a study on the growth of graphene thin films on a silicon substrate in a single step, using a graphite target and a pulsed laser. The study focused on the influence of substrate temperature (ST) on the deposition of graphene-like thin films using the pulsed laser deposition (PLD) technique. In the synthesis, a highly oriented pyrolytic graphite target was irradiated by the fundamental harmonic (1064 nm) of a Nd: YAG pulsed laser. Under the experimental conditions, a background gas pressure of 50 mTorr containing oxygen was used and the ablation time was 5 min. Both the background gas pressure condition and the ablation time were maintained the same for all samples and the only variable used in this study was the ST, which varied from room temperature (25 °C) to 500 °C. In order to study the morphological, structural, and chemical properties of the 4 samples grown, 6 characterization techniques were used. The samples were characterized by Raman spectroscopy, Fourier-transform infrared spectroscopy (FTIR), Field Emission Scanning Electron Microscopy (FESEM) in conjunction with Energy dispersive X-ray spectroscopy (EDS), Atomic force microscopy (AFM), and water contact angle

[1] Plasma, Laser y Aplicaciones (GPLA), Universidad Tecnológica de Pereira, Colombia – Profesor/investigador – hriascos@utp.edu.co

[2] Laboratorio de instrumentación y fotónica (LIF), Universidad Federal de Rio de Janeiro, Brasil –estudiante/investigador – juandlopezv94@gmail.com

measurement (WCAM). The characterization techniques used in the 4 synthesized samples allowed us to determine that graphene-like thin films were grown on a silicon substrate at 400 ºC and 500 ºC and that the samples grown at ST less than 400 ºC presented structures similar to amorphous carbon. From the results of the spectroscopy, it was concluded that both the degree of graphitization and the degree of oxidation was influenced by the ST. Finally, with the measurement of water contact angle, it was possible to determine that the graphene-type samples presented hydrophobicity and that amorphous carbon samples were hydrophilic.

Key words: amorphous carbon, graphene, Pulsed Laser Deposition and thin Films

Resumen

En este capítulo, presentamos un estudio sobre el crecimiento de películas delgadas de grafeno en sustrato de silicio en una única etapa, utilizando un blanco de grafito y un láser pulsado. El estudio se centró en la influencia de la temperatura del sustrato (TS) en la deposición de películas delgadas similares al grafeno utilizando la técnica de deposición por láser pulsado (DLP). En la síntesis, un blanco de grafito pirolítico altamente orientado fue irradiado por el armónico fundamental (1064 nm) de un láser pulsado Nd: YAG. En las condiciones experimentales, se utilizó una presión de gas de fondo de 50 mTorr que contenía oxígeno y el tiempo de ablación fue de 5 min. Tanto la condición de presión de gas de fondo como el tiempo de ablación se mantuvieron iguales para todas las muestras y la única variable utilizada en este estudio fue la ST, que varió desde temperatura ambiente (25 °C) hasta 500 °C. Para estudiar las propiedades morfológicas, estructurales y químicas de las 4 muestras crecidas se utilizaron 6 técnicas de caracterización. Las

muestras se caracterizaron por espectroscopia Raman, espectroscopia infrarroja transformada de Fourier (IRTF), microscopía electrónica de barrido de emisión de campo (MEB) junto con espectroscopia de rayos X de energía dispersiva (SED), microscopía de fuerza atómica (MFA) y medición del ángulo de contacto con el agua (MACA). Las técnicas de caracterización utilizadas en las 4 muestras sintetizadas permitieron determinar que las películas delgadas similares al grafeno fueron crecidas sobre sustrato de silicio a 400 ºC y 500 ºC y que las muestras crecidas a ST menores que 400 ºC presentaron una estructura similar al carbono amorfo. De los resultados de la espectroscopia se concluyó que tanto el grado de grafitización como el grado de oxidación fueron influenciados por la TS. Finalmente, con la medición del ángulo de contacto con el agua se pudo determinar que las muestras similares al grafeno presentaban hidrofobicidad y las muestras de carbono amorfo fueron hidrofílicas.

Palabras Clave: carbono amorfo, grafeno, deposición por láser pulsado y películas delgadas

Introduction

Carbon allotropes are one of the most studied and used materials in technology today due to their optical, mechanical, and electrical properties, which depend on the bond between carbons and the functional groups in their chemical structure. Among these allotropes can be mentioned as amorphous carbon (Blue et al., 2018), graphite (Murakami et al., 2019), carbon nanotubes (Omoriyekomwan et al., 2020), quantum dots, and graphene (Khan et al., 2020). In recent years, graphene has attracted the attention of researchers due to its properties such as transparency, high conductivity, strength, and thermal conductivity, properties commonly used in optoelectronic

sensing and energy applications. However, when graphene presents hydroxyl bonds in its chemical structure, it is called graphene oxide. Thus, other materials can bind to graphene oxide structure through hydroxyl groups, facilitating the detection of certain targets, such as proteins, bacteria, and pollutants (Priyadarsini et al., 2018; Tadyszak et al., 2018), making it more interesting in biomedical applications.

To synthesize graphene oxide, several chemical and physical techniques have been used, such as chemical vapor deposition (CVD) (Robinson et al., 2012), chemical synthesis (Singh et al., 2016), micromechanical exfoliation (Baqiya et al., 2020), physical vapor deposition (PVD) (Wu et al., 2020), epitaxial growth on some substrates (Yoon et al., 2013), pulsed laser ablation (PLD) (Lu et al., 2021; Blue et al., 2018; Abd Elhamid et al., 2017; Manikandan et al., 2014; Hemani et al., 2013; Wang et al., 2011; Cappelli et al., 2007;)(Baqiya et al., 2020; Omoriyekomwan et al., 2020; Priyadarsini et al., 2018; Singh et al., 2016), among other techniques.

PLD is a simple, cost-effective, and versatile technique that allows control of the morphology and thickness of thin films. Furthermore, this technique makes it possible to obtain doped structures or some types of complex alloys (Lancok et al., 2021; Lu et al., 2021; Spellauge et al., 2021; Manikandan et al., 2015; Manikandan et al., 2014), which is its main advantage. Due to the high energies of the ionized and ejected species in laser plumes, PLD samples can be synthesized at lower deposition temperatures compared to PVD techniques (Cheung, 1994). Another advantage of PLD is that it allows the deposition of nanostructures with the same stoichiometry as the target used in the process.

The quality of samples grown by PLD mainly depends on laser features, such as fluence, pulse duration, wavelength, and repetition rate. But also, the samples' quality depends on other

experimental conditions, such as target nature (stoichiometry), target-substrate distance, gas pressure, gas environment, deposition time, and substrate temperature (ST) (Blue et al., 2018). The roughness and thickness of the deposited film are affected by the spherical expansion of the plasma plume induced by the laser, which depends on the target-substrate distance, as the sample growth rate increases as the target-substrate distance decrease (Mostako & Khare, 2012).

Deposition control, in terms of stoichiometric and homogeneity, is possible when the plasma length is identical to the target-substrate separation distance (Popescu et al., 2011). But the background gas pressure also plays an important role in the crystallinity and stoichiometry of the samples, as they can be modified through the thermalization of the plume, so for example, to obtain oxidized species in the deposition, oxygen could be used as background gas (Sambri et al., 2016). The morphology, structure, and crystallinity of the deposited films are also strongly influenced by ST, which are fundamental for the formation of graphene oxide. Additionally, an increase in ST allows a better adhesion rate to the substrate, which affects the roughness and size of the deposited crystal (Abd Elhamid et al., 2017; Hemani et al., 2013; Wang et al., 2011; Cappelli et al. 2007).

For graphene growth by the PLD technique, several works have been reported using metallic catalysts to favor the growth of a few layers/multilayers of graphene and also to perform growth at relatively low temperatures (Abd Elhamid et al., 2017; Abd Elhamid et al., 2017; Ren et al., 2017; Xiangming et al., 2015; Hemani et al., 2013; Wang et al., 2011; Cappelli et al., 2007; Capelli et al., 2005 Cheung, 1994). In 2017, the growth of graphene thin films on a copper substrate (used as a catalyst) using the PLD technique was reported (Abd Elhamid et al., 2017). The authors grew graphene at a relatively low temperature of 500 °C, which was possible by the use of the catalyst. Another study reported the synthesis of a few layers of graphene on substrates of Ni, Cu, and Cu-Ni alloys (Abd Elhamid et al., 2017). Samples were deposited using a Nd:YAG pulsed

laser operating at a wavelength of 1064 nm. The authors' objective was to obtain graphene at relatively low temperatures using metallic catalysts. However, when using metallic catalysts in the synthesis, the cost increases and it becomes a more elaborate procedure that requires more than one step.

Accordingly, the objective of this research project was to study the influence of ST on the deposition of graphene oxide on Si (100) substrate without the use of metallic catalysts. In this work, we present the growth of carbon thin films using the fundamental harmonic (1064 nm) of a Nd:YAG pulsed laser, under constant oxygen pressure and at relatively low TS. All samples were deposited in one step.

Materials and methods

To carry out the synthesis, the highly oriented pyrolytic graphite target and the Si substrate were sonified to clean the impurities on their surface. In the experimental setup, a Nd:YAG pulsed laser was used, with a wavelength of 1064 nm, a repetition rate of 10 Hz, and energy per pulse of 200 mJ. A pressure of ~50 mTorr was generated by injecting O_2 (99.99% pure) into the vacuum chamber at a rate of 20 sccm. The ablation lasted 5 minutes (3000 shots) for each sample. The thin films were grown at relatively low ST at 25, 200, 400, and 500 °C. The experimental conditions used for the growth of each thin film are shown in Table 1.

In the experimental setup, the laser beam irradiated the graphite target at an angle of 45º relative to the position of the Si substrate (as seen in Figure 1). The target was relocated for each synthesis, allowing the laser beam to strike another position of the target. The target also was kept rotating during the deposition time. The target-substrate distance was the same for each synthesis.

Table 1

Experimental conditions for the synthesis

Sample	Temperature (ºC)	Pressure (mTorr)	Wavelength (nm)	Deposition time (min)
S1	500	50	1064	5
S2	400			
S3	200			
S4	25			

Figure 1

Experimental setup of the PLD system.

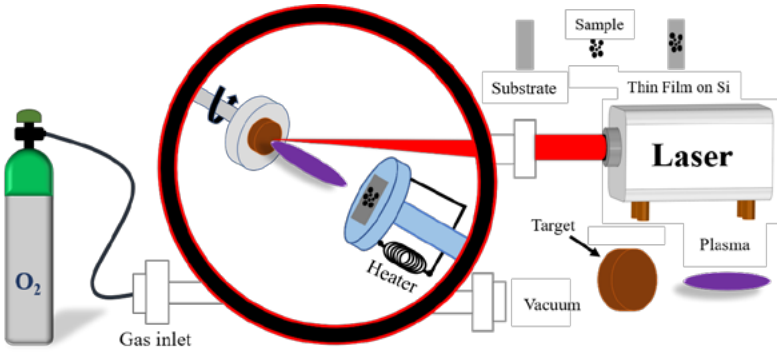

To characterize the thin films grown by PLD onto Si substrate, several techniques were used in order to study the structural, chemical, morphological, and surface properties. The samples were characterized by Raman confocal spectroscopy, Fourier transforms infrared spectroscopy (FTIR), Field Emission Scanning Electron Microscope (FESEM), X-ray Energy Dispersion Spectroscopy (EDS), Atomic Force Microscopy (AFM), and water contact angle measurement (WCAM).

Results and discussion

- *Raman confocal spectroscopy*

To investigate the influence of ST on the vibrational properties of the synthesized thin films, Raman spectroscopy was performed and the spectra are shown in Figure 2. All thin films were characterized from 1000 cm^{-1} to 3100 cm^{-1}.

In agreement with previous literature, all spectroscopic peaks observed can be assigned to peaks characteristic of thin films of carbon allotropes (Bhaumik et al., 2017; Ferrari, 2007; Ferrari & Robertson, 2000; Kumar et al., 2017; Roscher et al., 2019;). The results obtained from Raman show the presence of D, G, and 2D bands in samples S1 and S2, typical bands of graphene nanostructures. For S1, the D, G, and 2D bands are located around 1310, 1577, and 2755 cm^{-1}, respectively. For S2, these bands are located at approximately 1215, 1524, and 2755 cm^{-1}, respectively. On the other hand, samples S3 and S4 prepared at a lower ST presented a very wide band around 1450 cm^{-1}, with a weak shoulder around 1600 cm^{-1}, and furthermore, the 2D band does not appear in sample S3.

The D, G, and 2D bands are indicative of graphene film growth, their shapes, intensities, and locations indicate the "type" of synthesized carbon nanostructure (Lee et al., 2021; Thema et al., 2015; Krishnamoorthy et al., 2013; Yang et al., 2009). The D band is attributed to the in-plane breathing modes of sp^2 atoms in rings, which is associated with the disorder in the structure of the samples caused by certain defects such as grain boundaries, vacancies, and some species of a C. Intensity of D is also related to the size of the sp^2 domains and it is understood that when the D is absent there is the formation of perfectly crystalline graphene (Bhaumik et al., 2017; Krishnamoorthy et al., 2013). Likewise, the E_{2g} phonon mode in the Brillouin zone center corresponds to the G band (localized between 1520-1620 cm^{-1}), and it is associated with the bond stretching of sp^2 C atoms both for rings and chains (Ferrari, 2007). Furthermore, the degree of graphitization is attributed to the G band (crystalline quality) and it shows the formation of a hexagonal lattice in the graphite. Therefore, pure graphite presents a narrow and highly symmetric G peak, while wide and shifted towards a lower frequency corresponds to samples of amorphous carbon (a-C).

According to the Raman results, all samples present disorders related to different distributions of oxygen functional groups. The samples S3 and S4 (grown at low temperatures) presented an overlap of the D and G bands, which means the formation of a-C nanostructures, mainly for the S3 sample, where the 2D band does not appear (Wang et al., 2011). However, samples S1 and S2 presented the three typical bands of graphene, wide, asymmetric, and with a shift of its value assigned by the literature. The slightly blue shift in the spectra of the films compared to that of graphite, clearly reflect a structural change of the sp^2-C planes of the films and their predominantly graphene oxide (GO) formation.

The disorder degree can be calculated with the I_D/I_G ratio, being inversely proportional to the average size of the sp2 clusters, where I_G (I_D) is the intensity of the G (D) band. We calculated the I_D/I_G ratio in the GO structures from Raman results (Figure 2), which resulted in around 0.83 and 1.57 for S2 and S1, respectively, indicating that S2 presented fewer oxidized functional groups (Gupta et al., 2017). The I_D increase in S1 compared to S2 may be due to an increasing the ST which can generate a higher rate of deposited oxygen species, increasing the level of disorder in the sample structure. Also, increasing TS generates an increased rate of carbon deposition, and the disorder may be due to stacking between layers, or even due to atomic defects within layers.

The number of layers of graphene can be calculated using the I_{2D}/I_G ratio, although it is qualitative information. The I_{2D}/I_G ratio was 0.187 and 0.305 for S2 and S1, respectively. According to the literature, an I_{2D} / I_G ratio between 0.6-0.69 suggests the formation of few-layer of graphene (4-5 layers), and a ratio less than 0.6 suggests the formation of multi-layer graphene (> 5 layers) (Blue et al., 2018). Thus, the results obtained from Raman spectroscopy indicate that the samples S1 and S2 presented the formation of multilayer GO (Blue et al., 2018; Yang et al., 2009; Ferrari, 2007).

From Raman, the results allow us to conclude that in S3 and S4 there was no evidence of graphene deposition, and perhaps there was a growth of a-C in these samples.

Figure 2

Raman results of samples a) S1 and S2, and b) S3 and S4.

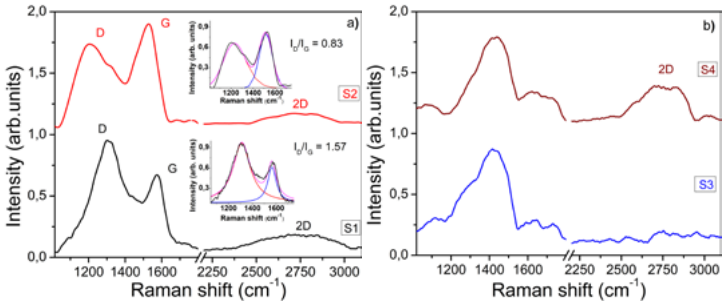

- *FTIR analysis*

FTIR results of the as-grown films are shown in Figure 3. The overall spectra of the samples S1 and S2 have similar characteristics to that of GO film determined in previous studies (Dimiev & Eigler, 2017; Shinohara et al., 2015; Mungse & Khatri, 2014), which agrees with Raman's analysis.

A wide variety of carbon-bound oxygen groups, typical of GO, rGO, and their functionalized forms are present in samples S1 and S2, as shown in Figure 3. It can be confirmed by the peak at 1109 cm^{-1} attributed to stretching vibrations of the epoxy group, at 1455 cm^{-1} (C-O-H, stretching vibrations of carboxyl), at 1638 cm^{-1} (C=C) it can be assigned to the non-oxidized graphitic domains, this due to the water molecules adsorbed on the surface of the films, at 1725 cm^{-1} (C=O, carbonyl) and at 3400 cm^{-1} (-OH, hydroxyl group) (Dimiev & Eigler, 2017; Gupta et al., 2017; Mungse & Khatri, 2014; Krishnamoorthy et al., 2013). In samples S1 and S2, a significant change in the intensity of the peaks is not observed. The oxidation degree is related to the intensity of these peaks, and their decrease indicates the elimination of oxygen-containing groups. Therefore, both samples (S1 and S2) have a similar degree of oxidation.

Unlike samples S1 and S2, the intensities of the peaks change in S3 and S4. For sample S4, some peaks disappear, indicating there are no non-oxidized graphitic domains (C=C). While in sample S3, the intensities of the peaks are weak.

Figure 3

FTIR results of samples S1, S2, S3 and S4.

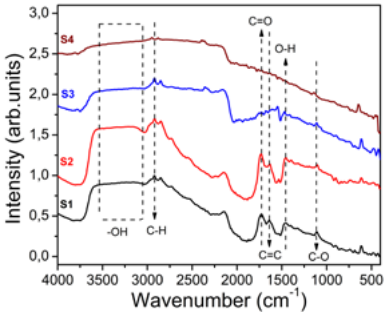

- *FESEM imagens*

The morphological properties of the thin films deposited were analyzed by FESEM and their results are shown in Figure 4(a-d). The images show a structure of dense and compact surfaces, composed of tubules with irregular shapes and intertwined with each other, containing small planes of layered graphene, which grow on a substrate structure to form a disordered solid, which is attributed to the formation of oxygen-containing functional groups and sp^3 carbons in the basal planes. The irregular and intertwined shapes in the structures suggest low oxygen content and the intercalation of oxygen atoms between the graphene layers (Mungse & Khatri, 2014).

Figure 4

FESEM images of samples a) S1, b) S2, c) S3, and d) S4.

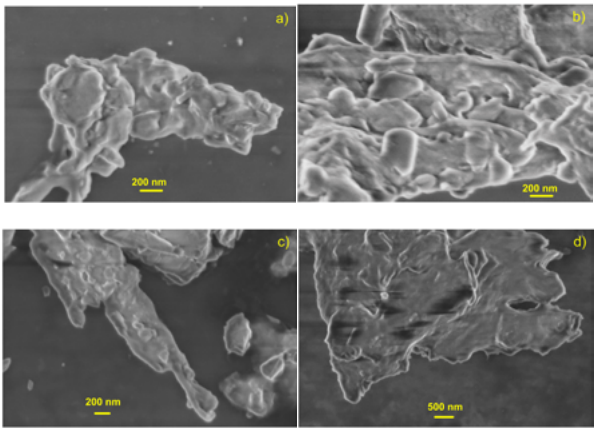

- *EDS analysis*

The elemental composition of each thin film was characterized by EDS (see Figure 5). The percentage of atomic oxygen in samples S1, S2, S3, and S4 was 4.50, 4.17, 3.81, and 3.78 (at. %) respectively, indicating low oxygen content in all samples, clearly confirming the previous analysis (Raman and FTIR). The low level of oxygen observed in samples, observed in Figure 5, is attributed to the oxygen background pressure used in the synthesis.

Figure 5

EDS spectra of samples a) S1, b) S2, c) S3, and d) S4

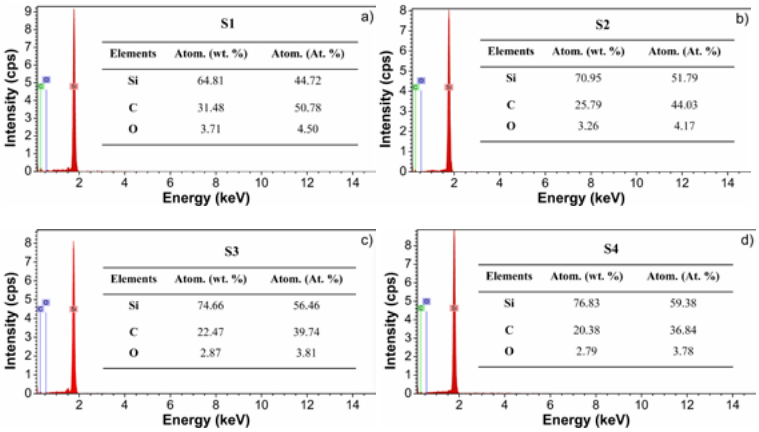

.

- *AFM images*

AFM images of the thin films deposited at different ST are shown in Figure 6. It was observed that there was no significant change in morphology with the change in ST. In order to determine the average grain size and roughness, an area of 3x3 μm was analyzed in each sample and the results were reported in Table 2.

The surfaces of these films appear continuous, although thick and rough, the individual flakes cannot be resolved, because it is not possible to distinguish their edges and there are extensive networks of long and wide wrinkles on the surface of the film. In general, we observe that the samples have a degree of disorder in their nanostructure, probably as a result of the rapid

dynamics of PLD and the flexible nature of GO sheets. The presence of covalently bonded oxygen atoms and the small up and downshift from the graphene original plane of sp^3 hybridized carbon atoms explain that GO sheets are thicker.

Table 2

Influence of ST on average grain size and roughness of the samples.

Sample	ST (ºC)	Average grain size (nm)	Roughness (nm)
S1	500	25 ± 10	3.0
S2	400	28 ± 12	5.1
S3	200	13 ± 7	2.1
S4	25	18 ± 10	3.4

Figure 6

AFM images of samples a) S1, b) S2, c) S3 and d) S4.

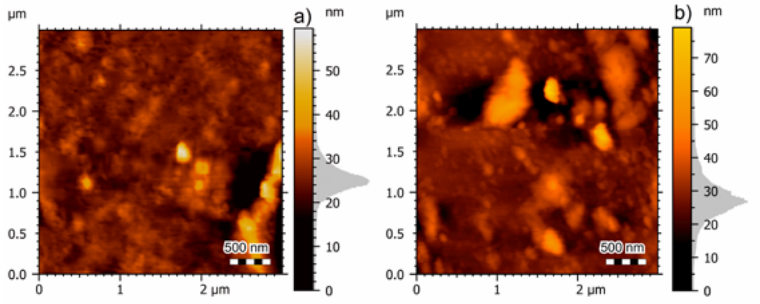

Inicio

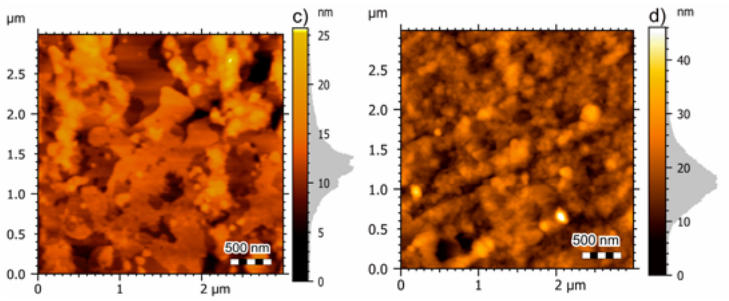

- *Contact angle measurement*

The surface wettability property is strongly influenced by the morphology and chemical composition of thin films, and this property can be studied through the water contact angle measurement (WCAM) (Poochai et al., 2019; Melios et al., 2018; Sadri et al., 2017; Bharathidasan et al., 2015). As the morphology and chemical composition were influenced by ST, then it is expected that the samples present different results.

The WCAM was carried out to study the wetting properties of all the thin films and its results are shown in Figure 7. The contact angle value of samples S1 and S2 was > 94º indicating the hydrophobic nature of the samples and in the literature, this value is associated with GO (Poochai et al., 2019; Melios et al., 2018; Sadri et al., 2017; Bharathidasan et al., 2015). Unlike S1 and S2, samples S3 and S4 exhibit angles less than 62º, which indicates hydrophilic properties for a-C thin films. Also, it was observed that the samples S2 have a greater contact angle than S1 (both GO), which is attributed to their oxygen content and their roughness, as verified with the characterization techniques used previously.

The results of the characterization techniques allowed us to determine that samples S1 and S2 presented a multilayer structure of GO, with a low degree of oxidation. It was also corroborated that ST strongly influenced both the crystallinity and the surface properties of the thin films deposited by PLD.

Given the synthesis conditions (ST >= 400 ºC) used for the growth of multilayer GO, we can propose this type of structure for several applications, among them, the measurement of polluting gases such as hydrogen sulfide (H2S) and/or, for coatings stainless steel used in the oil and gas industry to inhibit the deposition of calcium carbonate (CaCO3). Both applications are very important in the oil and gas industry, as H2S and CaCO3 are responsible for many economic losses in this industry (Lopez et al. 2021; Martinez et al. 2019). The functional groups (hydroxyl) present in the structure of multilayer GO and its hydrophobic properties make it a good candidate to be explored since this area requires both functionalize and hydrophobic materials.

Figure 7

Water contact angles of samples a) S1, b) S2, c) S3 and d) S4.

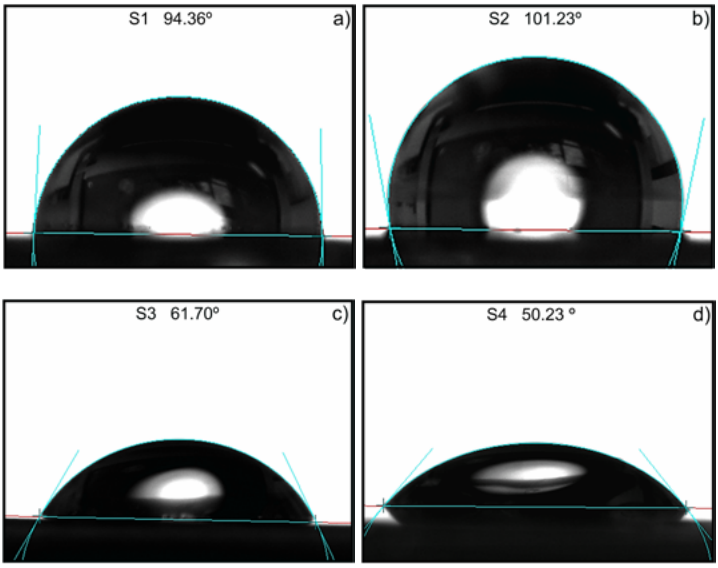

Conclusion

In this research project, the growth of carbon thin films in a single step using the PLD synthesis technique was proposed, with the objective of studying the influence of ST on the structural, chemical, and surface properties of thin films grown by PLD. Therefore, to carry out the study, 4 thin films were deposited onto a Si substrate varying the temperature from 25 to 500 ºC. Soon after, these films were characterized by Raman, FTIR, FESEM, AFM, and WCAM.

Raman results indicated that GO (multilayers) was deposited only in samples S1 and S2, which were grown in ST at 500 and 400 ºC, respectively. In agreement, FTIR results corroborated the presence of graphene with oxygen bonds in samples S1 and S2, likewise, for samples S3 and S4, the presence of a-C was confirmed. The oxygen level in the samples was also qualitatively analyzed using EDS characterization, which indicated that the samples presented an oxygen level of approximately 10% in relation to carbon.

AFM results show that samples S1 and S2 (GO) presented a higher average grain size than samples S3 and S4 (a-C). Furthermore, using WCAM it was found that the GO thin films were hydrophobic and that the a-C samples were hydrophilic.

Finally, we confirmed that ST played an important role in the structural, chemical, and surface properties of the samples. We also showed that it was possible to obtain graphene-like carbon without using metallic catalysts and in a single step.

Acknowledgments

This work was supported by *project research 3-21-2* from the Universidad Tecnológica de Pereira-Colombia.

References

Abd Elhamid, A. E. M., Hafez, M. A., Aboulfotouh, A. M., & Azzouz, I. M. (2017). Study of graphene growth on copper foil by pulsed laser deposition at reduced temperature. *Journal of Applied Physics*, *121*(2), 025303.

Abd Elhamid, A. M., Aboulfotouh, A. M., Hafez, M. A., & Azzouz, I. M. (2017). Room temperature graphene growth on complex metal matrix by PLD. *Diamond and Related Materials*, *80*, 162-167.

Baqiya, M. A., Nugraheni, A. Y., Islamiyah, W., Kurniawan, A. F., Ramli, M. M., Yamaguchi, S., ... & Cahyono, Y. (2020). Structural study on graphene-based particles prepared from old coconut shell by acid–assisted mechanical exfoliation. *Advanced Powder Technology*, *31*(5), 2072-2078.

Bharathidasan, T., Narayanan, T. N., Sathyanaryanan, S., & Sreejakumari, S. S. (2015). Above 170 water contact angle and oleophobicity of fluorinated graphene oxide based transparent polymeric films. *Carbon*, *84*, 207-213.

Bhaumik, A., Haque, A., Taufique, M. F. N., Karnati, P., Patel, R., Nath, M., & Ghosh, K. (2017). Reduced graphene oxide thin films with very large charge carrier mobility using pulsed laser deposition. *J. Mater. Sci. Eng*, *6*(4), 1-11.

Bleu, Y., Bourquard, F., Tite, T., Loir, A. S., Maddi, C., Donnet, C., & Garrelie, F. (2018). Review of graphene growth from a solid carbon source by pulsed laser deposition (PLD). *Frontiers in chemistry*, 6, 572.

Cappelli, E., Iacobucci, S., Scilletta, C., Flammini, R., Orlando, S., Mattei, G., Ascarelli, P., Borgatti, F., Giglia, A., Mahne, N., and Nannarone, S., (2005). Orientation tendency of PLD carbon films as a function of substrate temperature: A NEXAFS study. *Diamond and related materials*, *14*(3-7), 959-964.

Cappelli, E., Orlando, S., Servidori, M., & Scilletta, C. (2007). Nano-graphene structures deposited by N-IR pulsed laser ablation of graphite on Si. *Applied Surface Science*, *254*(4), 1273-1278.

Cheung, J. T. (1994). *History and fundamentals of pulsed laser deposition Pulsed Laser Deposition of Thin Films* ed DB Chrisey and G Hubler.

Dimiev, A. M., & Eigler, S. (Eds.). (2016). *Graphene oxide: fundamentals and applications*. John Wiley & Sons.

Dong, X., Liu, S., Song, H., Gu, P., & Li, X. (2015). Few-layer graphene film fabricated by femtosecond pulse laser deposition without catalytic layers. *Chinese Optics Letters*, *13*(2), 021601-021601.

Ferrari, A. C. (2007). Raman spectroscopy of graphene and graphite: Disorder, electron–phonon coupling, doping and nonadiabatic effects. *Solid state communications*, *143*(1-2), 47-57.

Ferrari, A. C., & Robertson, J. (2000). Interpretation of Raman spectra of disordered and amorphous carbon. *Physical review B*, *61*(20), 14095.

Gupta, B., Kumar, N., Panda, K., Kanan, V., Joshi, S., & Visoly-Fisher, I. (2017). Role of oxygen functional groups in reduced graphene oxide for lubrication. *Scientific reports*, *7*(1), 1-14.

Hemani, G. K., Vandenberghe, W. G., Brennan, B., Chabal, Y. J., Walker, A. V., Wallace, R. M., and Fischetti, M. V. (2013) Interfacial graphene growth in the Ni/SiO2 system using pulsed laser deposition. *Applied Physics Letters*, *103*(13), 134102.

Khan, Z. G., & Patil, P. O. (2020). A comprehensive review on carbon dots and graphene quantum dots based fluorescent sensor for biothiols. *Microchemical Journal*, *157*, 105011.

Krishnamoorthy, K., Veerapandian, M., Yun, K., & Kim, S. J. (2013). The chemical and structural analysis of graphene oxide with different degrees of oxidation. *Carbon*, *53*, 38-49.

Kumar, P., Kanaujia, P. K., Vijaya Prakash, G., Dewasi, A., Lahiri, I., & Mitra, A. (2017). Growth of few-and multilayer graphene on different substrates using pulsed nanosecond Q-switched Nd: YAG laser. *Journal of Materials Science*, *52*(20), 12295-12306.

Lancok, J., Novotny, M., Volfova, L., More-Chevalier, J., & Pereira, A. (2021). Effect of oxygen pressure on stoichiometric transfer in laser ablation of Pr3+ doped Gd2O3–Ga2O3 binary system. *Journal of Vacuum Science & Technology A: Vacuum, Surfaces, and Films*, *39*(4), 043403.

Lee, A. Y., Yang, K., Anh, N. D., Park, C., Lee, S. M., Lee, T. G., & Jeong, M. S. (2021). Raman study of D* band in graphene oxide and its correlation with reduction. *Applied surface science*, *536*, 147990.

Lu, Y., Huang, G., Wang, S., Mi, C., Wei, S., Tian, F., Li, W., Cao, H., and Cheng, Y. (2021). A review on diamond-like carbon films grown by pulsed laser deposition. *Applied Surface Science*, *541*, 148573.

Manikandan, E., Kennedy, J., Kavitha, G., Kaviyarasu, K., Maaza, M., Panigrahi, B. K., & Mudali, U. K. (2015). Hybrid nanostructured thin-films by PLD for enhanced field emission performance for radiation micro-nano dosimetry applications. *Journal of Alloys and Compounds*, *647*, 141-145.

Manikandan, E., Murugan, V., Kavitha, G., Babu, P., & Maaza, M. (2014). Nanoflower rod wire-like structures of dual metal (Al and Cr) doped ZnO thin films: Structural, optical and electronic properties. *Materials Letters*, *131*, 225-228.

Melios, C., Giusca, C. E., Panchal, V., & Kazakova, O. (2018). Water on graphene: review of recent progress. *2D Materials*, *5*(2), 022001.

Mostako, A. T. T., & Khare, A. (2012). Effect of target–substrate distance onto the nanostructured rhodium thin films via PLD technique. *Applied Nanoscience*, *2*(3), 189-193.

Mungse, H. P., & Khatri, O. P. (2014). Chemically functionalized reduced graphene oxide as a novel material for reduction of friction and wear. *The Journal of Physical Chemistry C*, *118*(26), 14394-14402.

Murakami, M., Tatami, A., & Tachibana, M. (2019). Fabrication of high quality and large area graphite thin films by pyrolysis and graphitization of polyimides. *Carbon*, *145*, 23-30.

Omoriyekomwan, J. E., Tahmasebi, A., Dou, J., Wang, R., & Yu, J. (2021). A review on the recent advances in the production of carbon nanotubes and carbon nanofibers via microwave-assisted pyrolysis of biomass. *Fuel Processing Technology*, *214*, 106686.

Poochai, C., Sriprachuabwong, C., Srisamrarn, N., Sudchanham, J., Mensing, J. P., Lomas, T., Wisitsoraat, A., and Tuantranont, A. (2019). Facial electrosynthesis of hydrophilic poly (aniline-co-p-phenylenediamine) nanostructures for high performance supercapacitor electrodes. *Journal of Energy Storage*, *22*, 116-130.

Popescu, A. C., Duta, L., Dorcioman, G., Mihailescu, I. N., Stan, G. E., Pasuk, I., Zgura, I., Beica, T., Enculescu, I., Ianculescu, A., and Dumitrescu, I. (2011). Radical modification of the wetting behavior of textiles coated with ZnO thin films and nanoparticles when changing the ambient pressure in the pulsed laser deposition process. *Journal of Applied Physics*, *110*(6), 064321.

Priyadarsini, S., Mohanty, S., Mukherjee, S., Basu, S., & Mishra, M. (2018). Graphene and graphene oxide as nanomaterials for medicine and biology application. *Journal of Nanostructure in Chemistry*, *8*(2), 123-137.

Ren, P., Pu, E., Liu, D., Wang, Y., Xiang, B., & Ren, X. (2017). Fabrication of nitrogen-doped graphenes by pulsed laser deposition and improved chemical enhancement for Raman spectroscopy. *Materials Letters*, *204*, 65-68.

Robinson, Z. R., Tyagi, P., Murray, T. M., Ventrice Jr, C. A., Chen, S., Munson, A., Magnuson, C. W., and Ruoff, R. S. (2012). Substrate grain size and orientation of Cu and Cu–Ni foils used for the growth of graphene films. *Journal of Vacuum Science & Technology A: Vacuum, Surfaces, and Films*, *30*(1), 011401.

Roscher, S., Hoffmann, R., & Ambacher, O. (2019). Determination of the graphene–graphite ratio of graphene powder by Raman 2D band symmetry analysis. *Analytical methods*, *11*(9), 1224-1228.

Sadri, R., Zangeneh Kamali, K., Hosseini, M., Zubir, N., Kazi, S. N., Ahmadi, G., Dahari, M., Huang, N. M., and Golsheikh, A. M. (2017). Experimental study on thermo-physical and rheological properties of stable and green reduced graphene oxide nanofluids: Hydrothermal assisted technique. *Journal of dispersion science and technology*, *38*(9), 1302-1310.

Sambri, A., Aruta, C., Di Gennaro, E., Wang, X., Scotti di Uccio, U., Miletto Granozio, F., & Amoruso, S. (2016). Effects of oxygen background pressure on the stoichiometry of a LaGaO3 laser ablation plume investigated by time and spectrally resolved two-dimensional imaging. *Journal of Applied Physics*, *119*(12), 125301.

Shinohara, H., & Tiwari, A. (2015). *Graphene: an introduction to the fundamentals and industrial applications*. John Wiley & Sons.

Singh, R. K., Kumar, R., & Singh, D. P. (2016). Graphene oxide: strategies for synthesis, reduction and frontier applications. *Rsc Advances*, *6*(69), 64993-65011.

Spellauge, M., Winter, J., Rapp, S., McDonnell, C., Sotier, F., Schmidt, M., & Huber, H. P. (2021). Influence of stress confinement, particle shielding and re-deposition on the ultrashort pulse laser ablation of metals revealed by ultrafast time-resolved experiments. *Applied Surface Science*, *545*, 148930.

Tadyszak, K., Wychowaniec, J. K., & Litowczenko, J. (2018). Biomedical applications of graphene-based structures. *Nanomaterials*, *8*(11), 944.

Thema, F. T., Beukes, P., Ngom, B. D., Manikandan, E., & Maaza, M. (2015). Free standing diamond-like carbon thin films by PLD for laser-based electrons/protons acceleration. *Journal of Alloys and Compounds*, *648*, 326-331.

Wang, K., Tai, G., Wong, K. H., Lau, S. P., & Guo, W. (2011). Ni induced few-layer graphene growth at low temperature by pulsed laser deposition. *Aip Advances*, *1*(2), 022141.

Wu, Y., Wang, S., & Komvopoulos, K. (2020). A review of graphene synthesis by indirect and direct deposition methods. *Journal of Materials Research*, *35*(1), 76-89.

Yang, D., Velamakanni, A., Bozoklu, G., Park, S., Stoller, M., Piner, R. D., ... & Ruoff, R. S. (2009). Chemical analysis of graphene oxide films after heat and chemical treatments by X-ray photoelectron and Micro-Raman spectroscopy. *Carbon*, *47*(1), 145-152.

Yoon, T. L., Lim, T. L., Min, T. K., Hung, S. H., Jakse, N., & Lai, S. K. (2013). Epitaxial growth of graphene on 6H-silicon carbide substrate by simulated annealing method. *The Journal of chemical physics*, *139*(20), 204702.

2 CAPÍTULO DOS

A note about the existence of second-kind periodic solutions in tricomi's equations

Una nota sobre la existencia de soluciones de segunda clase en una ecuación de tricomi

Daniel Cortés Zapata[1] and Alexander Gutiérrez Gutiérrez[2].

Abstract

This paper studies the existence of periodic solutions of a generalization of Tricomi's equation corresponding to Tricomi's ϕ-equation, dissipative and with constant forcing, where ϕ is a diffeomorphism. The study is done using perturbation methods, which considers the non-linear part as a positive perturbation $\epsilon << 1$ and studies the preservation of periodic solutions based on the case without disturbance. On the other hand, Melnikov's function is used to find the conditions under which homoclinic curves are preserved.

[1] Universidad Tecnológica de Pereira, docente departamento de matemáticas, danielcorteszapata@utp.edu.co.

[2] Universidad Tecnológica de Pereira, docente departamento de matemáticas, alexguti@utp.edu.co.

Key words: periodic Solution, second-kind periodic solution, average method, Melnikov's function.

Resumen

Este artículo estudia la existencia de soluciones periódicas de una generalización de la ecuación de Tricomi correspondiente a la ecuación ϕ de Tricomi, disipativa y con forzamiento constante, donde ϕ es un difeomorfismo. El estudio se realiza mediante métodos pertubativos, que considera la parte no lineal como una perturbación positiva $\epsilon << 1$ y estudia la conservación de soluciones periódicas basadas en el caso sin perturbación. Por otro lado, se usa la función de Melnikov se usa para encontrar las condiciones bajo las cuales se conservan las curvas homoclínicas.

Key words: solución periódica, soluciones corredoras, método de promedios, función de Melnikov.

Introduction

The forced pendulum equation is a paradigm in dynamic systems and has been widely studied with different techniques, for instance, a review of the State of the Art of global results (non-perturbative) of the forced pendulum equation can be found in (Mawhin, 2004). A classic example of such equations is the well-known Tricomi's equation (Tricomi, 1933) given by the second-order differential equation

$$(T) \qquad x'' + c\,x' + a\,sin\,sin\,(x) = b$$

where $b, a > 0$ and $c \geq 0$ are parameters related to force, amplitude and damping, respectively. It can be shown that equation (T) has no equilibria when $b > a$ but there are periodic solutions of the second-kind i.e. a solution x such that $x(t+T) = x(t) + 2\pi$ for some $T > 0$, that attracts all the other solutions. In Figure 1 it is shown an example of a solution that goes up to the second-kind periodic solution. Whereas, for $b < a$ there is equilibria and the existence of a constant $c_0(a, b)$ so that if $0 < c < c_0(a, b)$ there exists one running solution, and if $c > c_0(a, b)$ periodic solutions of the second-kind are destroyed in a homoclinic bifurcation and the equilibria become global attracting, see for instance the work of Tricomi (1933).

Figure 1

Existence of asymptotically stable running solution

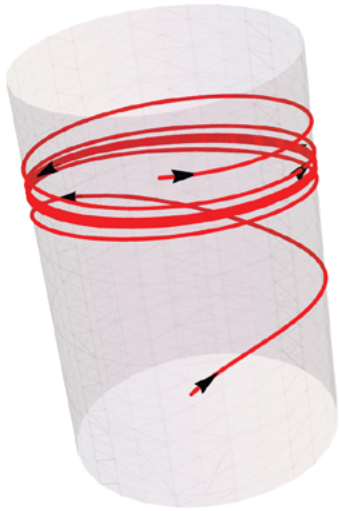

Source: own elaboration

We are interested in study conditions for the existence of second-kind periodic solutions for the Tricomi's generalized equation given by

$$(1) \qquad \left(\phi(x')\right)' + cx' + a\ sin(x) = b,$$

where $a, b > 0$, $c \geq 0$, and $\phi: I \to J$ is an increasing diffeomorphism, $0 \in I, J$ are open intervals in $\mathbb{R}$, $\phi(0) = 0$, ϕ could be a singular function or regular bounded or unbounded function, i.e.

- $\phi(x)$ is *singular*, this is, $I = (x_1, x_2)$ and $lim_{x \to x_i} \phi(x) = \pm\infty$, $i = 1,2$, or
- $\phi(x)$ is *regular no bounded,* this is $I = R$ and and $lim_{x \to \pm\infty} \phi(x) = \pm\infty$,
- $\phi(x)$ is *regular bounded,* this is $I = R$ and $lim_{x \to \pm\infty} \phi(x) \in R - \{0\}$.

Equation (1) type can be found in more physical applications such as relativistic flows, signal processing or epidemiology (Carapella, 2002). Some applications and studies can be found in the paper of Cabada et al. (2016). On the other hand, an interesting case can be found in the work of Torres (2008), who studied a relativistic pendulum where ϕ is given by

$$(P) \qquad \phi(x) := \frac{x}{\sqrt{1 - x^2}},$$

determining conditions under which there are periodic solutions using Schauder's fixed point Theorem. Some other studies of a relativistic pendulum can be found in Maro (2013) who establishes conditions for the existence of second-kind solutions where at least one of them is unstable, also established conditions on parameters for characterized isolated periodic solutions and their stability, by topological methods or in the work of Serna (2022) where the persistence of homoclinic is studied.

Gutierrez and Castro (2018) study the equation (1) when $c = 0$ (conservative case) determining the non-existence of second-class periodic solutions when $b < a$ and ϕ is singular or regular unbounded, while if $b \geq a$ there are no periodic solutions and if $b = a$ exist there is a unique point of equilibrium which is a cusp. Also, when $c > 0$ (dissipative case), they determine the existence, uniqueness, and asymptotic of a second-kind solution with $b/a > 1$, provided $(b + a)/c$ belongs to I.

We will prove the existence of a second-kind solution, in the case when c>0 and b<a using perturbation theory which is applied to non-linear oscillations and is based on a system where the solutions are known and a perturbation of this system is made, for instance, see Guckenheimer and Holmes (1986) or Verhulst (2007).

MATERIALS AND METHODS

To establish the condition for the existence of second-kind periodic solutions of (1) we use the perturbation theory. Firstly, we use the Average method to find conditions for the existence of either equilibria or running solutions, see Verhulst (2007) and Guckenheimer (1986). And second, we will use Melnikov's function, see Perko (2000) to establish conditions under the parameters to find the persistence of the homoclinic curve and then the existence of second-kind solutions.

RESULTS AND DISCUSSION

Main Results

For our study, it's necessary to modify equation (1) in two ways to apply perturbation methods. In the first way we apply Average, for that purpose we perturbed equation (1) as follows

$$(2) \qquad \left(\phi(x')\right)' + \epsilon(cx' + a\ sin(x) - b) = 0.$$

Based on the results of Verhulst (2007), we obtained Theorem 1.

Theorem 1. Given the differential equation (2) with $c > 0$ and $\phi \in C^3(I)$-diffeomorphism in a neighborhood of the point b/c then, (2) has an asymptotically stable periodic solution or a for ϵ small enough.

The previous theorem raises the existence of second-class periodic solutions regardless of the relationship between a and b, however, as proposed by Gutierrez and Castro (2018), if $b > a$, there always exists a single periodic solution of the second-kind, but there is no characterization of these when $b < a$. Theorem 1 guarantees the existence of either an equilibrium point or a running solution regardless of the relationship between a and b. However, to characterize in which cases there are periodic second-kind solutions when $b < a$, it is pending to resolve.

To achieve such characterization, we use Melnikov's function and modify equation (1) in the following way

$$(3) \qquad \left(\phi(x')\right)' + a\ sin(x) + \epsilon(cx' - b) = 0.$$

Note that when $\epsilon = 0$, equation (3) has two heteroclinic orbits for the fixed points $(\pm\pi, 0)$ as long as

$$(C1) \qquad \int_0^{y_2} s\,\phi(s)\,ds, \int_0^{y_1} s\,\phi(s)\,ds > 2a,$$

where $\$\phi: [y_1, y_2] \rightarrow R\$$ with $y_1 \leq 0 \leq y_2$. Now, denote the upper and lower heteroclinic as Γ^+ and Γ^- respectively and define the values

$$\xi_1 = \int_{-\pi}^{\pi} \frac{dx}{\phi'\left(\psi^{-1}(a + (x))\right)}, \qquad \xi_2 = \int_{-\pi}^{\pi} \frac{\psi^{-1}(a + acos\,(x))}{\phi'(\psi^{-1}(a + acos\,(x)))} dx,$$

Where

$$\psi(y) = \int_0^y w\, \phi'(w) dw.$$

We have the following theorem that establishes the persistence of the upper heteroclinic.

Theorem 2. Given the conditions of (C1) and set ξ_1 , ξ_2 as before, with $0 < b < a, c > 0$, then the orbit Γ^+ persist as long as ϵ is sufficiently small and:

$$(C2) \qquad \frac{b}{c} \approx \frac{\xi_2}{\xi_1}.$$

It can be shown that only the superior heteroclinic can persist, while the inferior one always breaks. The persistence and rupture of homoclinic and heteroclinic, which studies Melnikov's function, allows the detection of the appearance of chaos in the systems, see Guckenheimer (1986). Also, it is possible to verify that if the Melnikov function is positive then the stable manifold is above the unstable, for this case we have the following corollary.

Corollary 1. Given the conditions of the hypothesis of Theorem 3 and in addition

$$\frac{b}{c} > \frac{\xi_2}{\xi_1}.$$

then, there exists a second-kind periodic solution of the equation of (3).

Sketches of the proofs

Sketch of proof Theorem 1. The proof is based on Verhulst (2007, Theorem. 11.5):

Auxiliary Theorem 1. Consider equation

$$x' + \epsilon f(t,x) + \epsilon^2 g(t,x,\epsilon) = 0, \quad (4)$$

and

- The vector functions $\$f, g, \partial f/\partial x, \partial^2 f/\partial x^2, \partial g/\partial x$, are defined, continuous, and bounded by a constant M (independent of ϵ) in $[0,\infty] \times D$, $0 \le \epsilon \le \epsilon_0$ and
- f and g are T-periodic in t (T independent of ϵ).

If p is a critical point of the averaged equation whereas

$$\left|\frac{\partial f^0(y)}{\partial y}\right|_{y=P} \neq 0,$$

then, there exists a T-periodic solution $\varphi(t,\epsilon)$ which is close to p such that

$$\varphi(t,\epsilon) = p$$

And taking (Verhulst, 2007, Theorem. 11.6):

Auxiliary Theorem 2. Suppose that the conditions of Auxiliary Theorem 1 have been satisfied. If the eigenvalues of the critical point y=p all have negative real parts, the corresponding periodic solution $\varphi(t,\epsilon)$ is asymptotically stable for ϵ sufficiently small. If one of the eigenvalues has a positive real part, $\varphi(t,\epsilon)$ is unstable.

In our case we take:

$$f^0(y) = \int_0^{2\pi} \frac{-cy - (x) + b}{y\phi'(y)}\, dx = \frac{b - cy}{y\phi'(y)},$$

and note that the function $f(x, y) = \frac{-cy - a\sin x + b}{y\,\phi'(y)}$ is defined for all y in a neighborhood of the point b/c, and since it is continuous in a compact, we can define a constant M that bounded this function. Moreover, since $\phi'(y)$ is always positive in the neighborhood, the function is well-defined and its derivatives with respect to x exist and are continuous.

Sketch of proof Theorem 2

The idea is to know when Γ_β persists in (3), when $0 < \epsilon << 1$, i.e. if $\Gamma_\beta(t, \epsilon)$ is homoclinic of (3) generated by Γ_β. The first approximation of $\Gamma_e(t, \epsilon)$ (t, is given by the zeros of Melnikov's function $M_e(t)$ defined as:

$$M_e(t) := \int_{H(x_1, x_2) = e} g_2 dx_1 - g_1 dx_2$$

For that purpose, we use the next auxiliary theorem due to Han et al. (2012, Theorem 6.4).

Auxiliary Theorem 3. Suppose $e_0 \in]\alpha, \beta]$ and $t_0 \in R$. Then:

- If $M_{e_0}(t_0) \neq 0$, then, there are no limit cycles near Γ_{e_0} for $\epsilon + |t_0 + t|$ sufficiently small.
- If $M_{e_0}(t_0) = 0$ is a simple zero there is exactly one limit cycle $\Gamma_{e_0}(t_0, \epsilon)$ for $\epsilon + |t_0 + t|$ sufficiently small that approaches Γ_{e_0} when $(t, \epsilon) \to (t_0, 0)$.

Melnikov's function can be interpreted as the first approximation in ϵ of the distance between the stable and unstable manifold, measured along the perpendicular direction to the undisturbed connection, that is

$$d(\epsilon) := \epsilon \frac{M_{\beta(t_0)}}{\left|\left|f(\gamma_\beta)\right|\right|} + O(\epsilon^2)$$

In particular, when $M_{\beta(t_0)} > 0$ (resp. <0) the unstable manifold is above (resp. below) the stable manifold, see for instance Guckenheimer and Holmes (1986).

In our case, we have that

$$M_\beta(t_0) = b\xi_1 - c\xi_2,$$

which has simple zeros when

$$\frac{b}{c} \approx \frac{\xi_2}{\xi_1}.$$

CONCLUSIONS.

- Perturbation methods allow the establishment of local conditions on the parameter to determine the existence of both equilibria and running solutions for the equation (1), therefore, this method can be used to approach numerically those solutions.

- The technique used can estimate locally the existence of regions where only exist running solutions, only a fixed point, and the existence of both, running and fixed points, given conditions where there are bifurcations curves.

REFERENCES

Cabada A., and Fernández, F. A. (2016). Periodic solutions for some phi-Laplacian and reflection equations. *Boundary Value Problems*, 2016, 1-16

Carapella, G., Costabile, G., Martucciello, N., et al. (2002). Experimental realization of a relativistic fluxon ratchet, 382, 337–341.

Guckenheimer J. and Holmes P. (1986). *Nonlinear Oscillations, Dynamical Systems, and Bifurcations of Vector Fields*, Springer.

Gutierrez A. and Castro D. A. (2018). La phi-ecuación de Tricomi. *Ingeniería Y Ciencia, Fondo Editorial Universidad EAFIT*, 14, fasc.27. 11-28.

Han M. and Yu, Pu, (2012). *Normal Forms, Melnikov Functions, and Bifurcations of Limit Cycles*. Springer.

Marò, S., (2013). Periodic solutions of a forced relativistic pendulum via twist dynamics. *Topol. Methods Nonlinear Anal*, 42, 51-75.

Mawhin J. (2004). *Handbook of Differential Equations: Ordinary Differential equations.* Elsevier, vol. 1, ch. *Global results for the Forced Pendulum Equation*. 533–589.

Perko, L. (2000). *Differential Equations and Dynamical Systems*. Third Edition, Springer.

Serna, J. C. (2022). *Análisis cualitativo de un modelo asociado a una partícula relativista con amortiguamiento y forzamiento externo* [Tesis de Maestría]. Universidad Tecnológica de Pereira.

Torres, P. J. (2008). Periodic oscillations of the relativistic pendulum with friction. *Physics Letters A*. 372 6386-6387.

Tricomi, F. (1933). Integrazione di un'equazione differenziale presentatasi in elettrotecnica. *Annali della Scuola Normale Superiore di Pisa- Classe di Scienze*, 2, 1–20.

Verhulst, F. F., Sanders J.A. and Murdock J. (2007). *Averaging Methods in Nonlinear Dynamical Systems,* Second Edition, Applied Mathematical Sciences, Vol 59, Springer.

3 CAPÍTULO TRES

Basic descriptive geometry with AUTOCAD

Geometría descriptiva básica con AUTOCAD

Alberto García López[1]

Abstract

This work provides a solution to the traditional way of understanding and teaching basic Descriptive Geometry and at the same time streamlines both the teaching and the way to solve the problems.

This work allows the replacement of traditional instruments such as set squares, pencils, scales, compasses, protractors, etc., which generally make slow and inaccurate solutions, with software that provides an agile environment to solve the problems.

This software is not intended to teach and replace the teacher, nor to automatically solve the problems since it is the user who will continue to give the solutions through the commands, it is only intended to streamline and facilitate the tracing and development of the different procedures and methods used in basic Descriptive Geometry.

Keywords*:* descriptive geometry, teaching, AutoCAD, AutoLISP.

[1] Msc. Departamento De Dibujo, Facultad de Ciencias Básicas, Universidad Tecnológica de Pereira, nalan@utp.edu.co

Resumen

Esta obra aporta una solución a la forma tradicional de entender y enseñar la Geometría Descriptiva básica y al mismo tiempo agiliza tanto la enseñanza como la forma de resolver los problemas.
Esta obra permite sustituir los instrumentos tradicionales como escuadras, lápices, escalas, compases, transportadores, etc., que generalmente realizan soluciones lentas e inexactas, por un software que proporciona un entorno ágil para resolver los problemas.

Este software no pretende enseñar y sustituir al profesor, ni resolver automáticamente los problemas ya que es el usuario quien seguirá dando las soluciones a través de los comandos, solo pretende agilizar y facilitar el trazado y desarrollo de los diferentes procedimientos y métodos utilizados en la Geometría Descriptiva básica.

INTRODUCTION

The current development of 3D CAD software makes us believe that it is possible that traditional descriptive geometry loses validity as a tool for analysis and solution of the different problems of this area of engineering, “Some say that geometry descriptive is no longer important because CAD/CAM is replacing it” (Universidad privada del Norte). This work allows an alternative and updated solution, since it uses the benefits of a platform such as the AutoCAD program, adding all the new commands specific to this solution.

The software uses the geometric tools contained in the AutoCAD program, allowing users in general, to replace all procedures and methods of tracing, with a series of additional commands

in the AutoCAD environment, these are performed with the quick and efficient precision of a computer, allowing the user to dedicate himself to the analysis and solution of such problems, without worrying about the problems of tracing with traditional instruments.

The work of teachers, students, architects, and engineers with descriptive geometry currently require the use of modern tools for the solution of this type of problem, this work allows us to give a solution to this difficulty.

In recent years there have been different attempts to solve and modernize the solution methodologies that involve descriptive geometry problems, for example, "change the design of manually solved Descriptive Geometry exercises to an automated process using High-Level CAD Templates" (Moreno Cazorla, 2017). As well as with the advance of the different solid modeling software, it seems that it makes unnecessary the traditional solution techniques of descriptive geometry.

This work wants to provide a solution to this problem, where the AutoCAD program platform is used, which is a widely used program for the development of new solutions, taking advantage of its characteristics in both 2D and 3D, as well as its ease for a combined work.

A set of routines expressed in new commands were performed in a work environment within the AutoCAD software, where the user finds most of the procedures that are used in the process of plotting and solving descriptive geometry problems. In addition, this Autolisp software, developed in the AutoCAD environment, can be used within the Windows and Mac OS operating systems.

All these methods and procedures are projected in a two-dimensional environment, similar to those that traditional Descriptive Geometry uses, the work was also complemented with the

realization of commands that allow the presentation of situations and solutions in 3D, which facilitates the understanding and final analysis of the different problems.

Materials and methods

The method used was to use the Autolisp language, a subset of the object-oriented [3-8] language LISP, which is used within the Autocad program, each activity of the Descriptive Geometry work process was replaced by a routine that in the program works as new commands added to the base program, a custom menu was also designed where all these new commands were presented in an orderly and grouped way.

Everything concerning the management of the nomenclature was integrated into the routines, and management of the different types of lines was also established to facilitate the visualization and understanding of the problems; a suitable working environment was also defined within the AutoCAD program, format selection, scales, letter, etc.

Subroutines were developed one by one and optimized for each particular case. Drawing of lines rotation, location of points, projection of points, lines and planes, measurement and drawing of lines given the true length and slope, measurement and tracing of the course of the lines.

Special routines were added for 2D work with the development of surfaces of basic elements. Finally, routines of 3D representation of what is done in 2D were developed, for almost all possible situations of Descriptive Geometry. The different subroutines were verified and tested for debugging and correction.

Results and discussion

The following objectives were met:

1. Design of routines that replace the process of tracing the different procedures:

- Drawing the line of rotation 1-2.

This line is drawn in two steps, as shown in Figure 1 with its respective nomenclature.

Figure 1

- Projection of points in two different projection planes as shown.

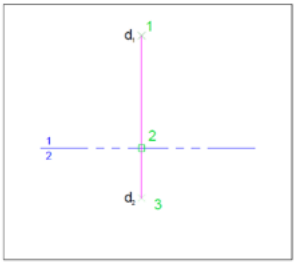

Projection of points in two different projection planes as shown.

Figure 2

- Projection of points with their respective nomenclature.

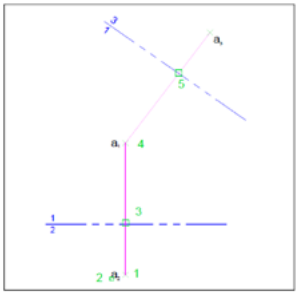

Here one of the basic rules of descriptive tracing is used, distance entering a projection plane, distance leaving.

Figure 3

Listing of the program of the “Projection of points” routine in Autolisp language

```
(defun C:ProyPun (/ tras aa lyn nom pln bb longitud cc dd alpha ubi ep ins1 ins3)
 (init)
 (setvar "osmode" 9)
 (setvar "snapmode" 0)
 (setq aa (getpoint "\nSeleccione punto de arranque de distancia a transferir: "))
 (princ "\nSeleccione la nomenclatura del punto:")
 (setq lyn (entget (ssname (ssget "_:S+.") 0)))
 (setq nom (cdr (assoc 1 lyn)))
 (initget 1 "1 2 3 4 5 6 7 8 9 10")
 (setq       pln (getkword "\n Designe la nomenclatura del punto destino
  [1/2/3/4/5/6/7/8/9/10]: " ) )
 (setvar "osmode" 128)
 (setq bb (getpoint aa "\n Seleccione la linea de giro: "))
 (setq longitud (distance aa bb))
 (setvar "osmode" 129)
 (setq cc (getpoint "\n Seleccione punto a ser proyectado: "))
 (setvar "osmode" 128)
 (setq dd (getpoint cc "\n Seleccione la otra linea de giro: "))
 (initget 1 "Si No")
 (setq tras (getkword "\n Existe traslape de puntos[Si/No]: "))
 (if (= tras "No")
   (progn (setq alpha (angle cc dd)))
   (progn (setq alpha (+ (angle cc dd) pi)))
 )
 (setq ep (polar dd alpha longitud))
 (setvar "osmode" 0)
 (command "_-layer" "_s" "0" "")
```

```
(command "_point" ep)
(initget 128)
(setvar "osmode" 0)
(setq       ubi(getkword"\n Indique la ubicación de la nomenclatura
 [N/NO/O/SO/S/SE/E/NE]:") )
(setq ubi (strcase ubi))
(cond
  ((= ubi "N") (progn (setq ins1 (polar ep 2.11 3.7))))
  ((= ubi "NO") (progn (setq ins1 (polar ep 2.82 5.6))))
  ((= ubi "O") (progn (setq ins1 (polar ep 3.38 7.0))))
  ((= ubi "SO") (progn (setq ins1 (polar ep 3.9 7.5))))
  ((= ubi "S") (progn (setq ins1 (polar ep 4.43 6.9))))
  ((= ubi "SE") (progn (setq ins1 (polar ep 5.01 5.5))))
  ((= ubi "E") (progn (setq ins1 (polar ep 5.76 3.5))))
  ((= ubi "NE") (progn (setq ins1 (polar ep 0.82 2.3))))
)
(setq ins3 (polar ins1 5.96 3.0))
(command "_-layer" "_s" "Nomenclatura" "")
(command "_text" ins1 4.0 0 nom)
(Command "_text" ins3 1.8 "" pln)
(command "_-layer" "_s" "Proyecciones" "")
(setvar "osmode" 0)
(command "_line" cc ep "")
(command "_-layer" "_s" "0" "")
(reset)
(setvar "snapmode" 1)
(princ)
)
```

(setfunhelp "c:ProyPun" "Ayuda Descriptiva" "proyección_de_puntos")

- Drawing parallel rotation lines.

- Drawing perpendicular rotation lines.

- Drawing lines with a given course.

- Measurement of the course of a line.

- Line drawing given slope and length.

- Measurement of slope and length.

2. Design of complementary routines, which allow an adequate display of the solution and understanding of the same in 3D.

- Plotting of points, lines, and planes in 3D and their projection in horizontal and frontal views.

- 3D projection of the different auxiliary elevation projection planes.

- 3D projection of the different auxiliary inclined projection planes.

3. Special routines for 2D surface development:

- Extension of the perimeter of the straight section of a prism or cylinder.

- Drawing of longitudinal edges, perpendicular to the straight section perimeter.

- Location of intermediate points in the development of prisms and cylinders.

- True length by rotation.

- Copying figures by triangulation.

- Location of intermediate points in pyramids and cones.

4. Perform automated integration and installation as a website application. AUTODESK EXCHANGE APPS.

Conclusions

The solution given with this software allows effectively to speed up the operative work that otherwise, either with traditional instruments or with the different types of basic CAD software do not allow dynamic and agile work, actually, sometimes this seems to slow it down.

The different routines allow the elaboration and location of the standardized nomenclature in an easy and logical way, allowing this task, firstly, not to be forgotten and secondly, to be easy and agile.

Secondly, the solution given to the 3D representation of the different problems allows to spatially understand all types of problems for both an explanation in a classroom or virtual classroom.

A group of specialized routines has also been added for the operative and repetitive work that has to be done for the elaboration of surface development.

Figure 4 shows the 19 additional commands grouped by functionality in the program's ribbon and in the two new toolbars, as well as two groups of commands in the menu area.

The software effectively allows the plotting time used in the different methods and procedures to be shortened by approximately 50%, specifically in the two-dimensional plotting methods, and this has to do specifically with the location of the nomenclature and with the agility of the projections of the different points.

As for the explanations with the help of the graphs generated in three dimensions, the agility and flexibility of this type of graphs are incalculable, as well as the time saving and the increased clarity that is produced by using the software.

This benefit of the agility and clarity obtained with the software is observed in the students, as they are the ones using the application.

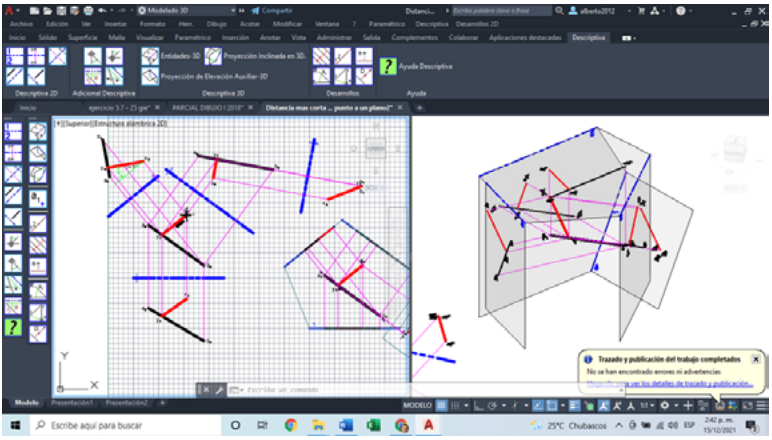

Figure 4

REFERENCES

Autodesk. (2023, 1 de marzo).AutoLISP Developer's Guide (AutoLISP). https://help.autodesk.com/view/ACD/2022/ENU/index.html?guid=GUID-265AADB3-FB89-4D34-AA9D-6ADF70FF7D4B

Autodesk. (2023, 1 de marzo). *About AutoLISP Data Types (AutoLISP)*. http://knowledge.autodesk.com/support/autocad/getting-started/caas/documentation/ACD/2013/ENU/files/GUID-7E568541-F1D0-49C4-B878-15880486825F-htm.html

García López, A. (2011) *Herramientas en Autocad para el desarrollo de superficies básicas*, Manual del usuario, UTP, Colombia.

López, J. Tajadura Zapirain, J. A. (1998) *Autocad Avanzado*. McGraw-Hill Interamericana

Moreno Cazorla, R. (2017). Automatización en la enseñanza de Geometría Descriptiva y CAD = Automation in the teaching of descriptive geometry and CAD. Advances in Building Education. 1. 40. 10.20868/abe.2017.2.3560. https://www.researchgate.net/publication/322793905_Automatizacion_en_la_ensenanza_de_Geometria_Descriptiva_y_CAD_Automation_in_the_teaching_of_descriptive_geometry_and_CAD

Tajadura Zapirain, J. A., Manso Irurzun, B., López Fernández J. (1999) *Programación con Autocad*, McGraw Hill.

Universidad privada del Norte. (2023, 1 de marzo). Geometría descriptiva y software CAD/CAM. https://blogs.upn.edu.pe/ingenieria/2015/05/25/geometria-descriptiva-y-software-cadcam/

Desde nuestra Facultad se presentan trabajos resultados de investigación que le aportan significativamente a las aplicaciones de las ciencias básicas y que son el resultado del compromiso y la dedicación de nuestros docentes investigadores, quienes trabajan para abordar problemas complejos y generar soluciones innovadoras y sostenibles.

En el primer capítulo se presenta un estudio de las propiedades en nuevos materiales, en este caso del crecimiento de películas delgadas de grafeno en sustrato de silicio utilizando el método de deposición por láser pulsado (DLP) donde se utilizaron 6 técnicas de caracterización (Espectroscopía Raman, IRTF, MEB, SED, MFA, MACA) y como conclusión se tiene que las muestras similares al grafeno presentan propiedades de hidrofobicidad y las muestras de carbono amorfo tienen propiedades hidrofílicas.

En el segundo capítulo se presenta un modelamiento matemático y una discusión sobre la existencia de soluciones de segunda clase en una ecuación de Tricomi, se plantea la existencia de soluciones periódicas de una generalización de la ecuación de Tricomi, el estudio se realiza mediante métodos perturbativos; de igual forma, se usa la función de Melnikov para encontrar las condiciones bajo las cuales se conservan las curvas homoclínicas.

En el tercer capítulo se plantea una metodología de enseñanza-aprendizaje para enseñar la geometría descriptiva básica y la resolución de problemas a través del software Autocad.

Se agradece a todos los docentes, estudiantes, equipos de trabajo y colaboradores de la Facultad de Ciencias Básicas y a la Vicerrectoría de Investigaciones, Innovación y Extensión, por seguir aportando a la construcción y fortalecimiento de la ciencia, la tecnología y la innovación, a mejorar los procesos de formación y la aplicabilidad de las ciencias en diversos ámbitos y que impactan sin duda a una sociedad del conocimiento.

Vicerrectoría de Investigaciones, Innovación y Extensión
Facultad de Ciencias Básicas
Colección Trabajos de Investigación

eISBN 978-958-722-805-2